Theoretical & Applied Mechanics Letters 10 (2020) 390-404

Contents lists available at ScienceDirect

Theoretical & Applied Mechanics Letters

journal homepage: www.elsevier.com/locate/taml

Letter

# Efficient model for the elastic load of film-substrate system involving imperfect interface effects

Wenwang Wu[a,b], Huabin Yu[b], Rui Xue[b], Tian Zhao[b], Ran Tao[b,*], Haitao Liao[b,*], Zhongdong Ji[c]

[a] School of Naval Architecture, Ocean and Civil Engineering, Shanghai Jiao Tong University, Shanghai 200240, China
[b] Institute of Advanced Structure Technology, Beijing Institute of Technology, Beijing 100081, China
[c] Institute of Mechanics, Chinese Academy of Sciences, Beijing 100190, China

## HIGHLIGHTS

- Efficient calculation method is developed for elastic boundary load of film-substrate system.
- Three types of imperfect interface models are developed and verified.

## ARTICLE INFO

*Article history:*
Received 15 June 2020
Accepted 19 June 2020
Available online 19 June 2020
This article belongs to the Solid Mechanics.

*Keywords:*
Film-substrate
Imperfect interface
Elastic field

## ABSTRACT

In this paper, an efficient calculation method based on discrete Fourier transformation is developed for evaluating elastic load induced elastic deformation fields of film-substrate system. Making use of 2D discrete Fourier transformation, the elastic fields induced by Hertz load is harvested in frequency domain, and the displacement and stress fields across the interface are enforced to satisfy the elasticity conditions for each Fourier modes. Given arbitrary distributed stress field at free surface plane of the three types of film-substrate systems, unique resultant elastic field within the can be harvested. Hertz load of half space, elastic film on elastic substrate, elastic film on rigid substrate system and elastic film-substrate system with three types of imperfect interface models are investigated: (1) the spring-like imperfect interface model which can be described as: $u_k^f\big|_{z^f=-h} - u_k^s\big|_{z^s=0} = \boldsymbol{K}_T\sigma_{kz}$ and $u_z^f\big|_{z^f=-h} - u_z^s\big|_{z^s=0} = \boldsymbol{K}_N\sigma_{zz}$; (2) the dislocation-like interface model, where interface displacement and stress components relation can be described as: $u_i^f\big|_{z^f=0} = \boldsymbol{k}_{ij}^u\, u_i^s\big|_{z^s=0}$ and $\sigma_{iz}^f\big|_{z^f=0} = \sigma_{iz}^s\big|_{z^s=0}$; (3) the force-like interface model, where interface displacement and stress components relation can be described as: $u_i^f\big|_{z^f=0} = u_i^s\big|_{z^s=0}$ and $\sigma_{iz}^f\big|_{z^f=0} = \boldsymbol{k}_{ij}^t\,\sigma_{iz}^s\big|_{z^s=0}$ respectively. Finally, several simulation examples are performed for verification of the reliability and efficiency of the proposed semi-analytical methods.



Mechanical contact induced structural failure problems are of critical important in many industrial systems, such as: train wheel-rail system, transmission, cylindrical and planetary gearing, bearing components, and coating systems. These industrial components and systems have to endure various types of external mechanical, thermal loadings, harsh physical and chemical coupled environments during their service lifetime, and classic film-substrate design strategies are widely employed for improving their comprehensive mechanical performances. As to the interface properties of film-substrate system, bimaterial system and multi-layered structures, classical perfect bonding interface model is employed for studying the mechanical behaviors of these systems under external loading, where the interface traction stress and displacement components are continuous across the material interface. Although the perfect bonding interface model is convenient for theoretical understanding the mechanical behaviors of these integrated systems, it is not precisely val-

* Corresponding author.
*E-mail address:* taoran@bit.edu.cn (R. Tao), liaoht@bit.edu.cn (H.T. Liao).

http://dx.doi.org/10.1016/j.taml.2020.01.048

id for industrial structures in service. There are various types of imperfect mechanical interfaces during the service lifetime of film-substrate system, and investigation of the mechanical behaviors of film-substrate systems under external boundary load conditions is important for understanding the durability, reliability of these structural components and systems. In reality, perfect interface mechanical continuity is inadequate for precisely description of interface damage (e.g. de-bonding, sliding and/or cracking across an interface), since it is well-known that imperfect bonding along a material interface can significantly influence its mechanical and thermal properties [1]. Regarding to the relation between interface displacement and traction stress components across the imperfect interface, four types of classic interface models are proposed for describing the interface physical properties, namely: the classical perfect bonding model, the frictionless imperfect interface model, the dislocation-like imperfect interface model, and the force-like imperfect interface model [2–12].

Exact elastic fields analytical solutions of layer-substrate system are proposed by Chen [13]. Mixed boundary value problem in a multilayer medium is analyzed based upon classical elasticity theory, and comparison with classic Boussinesq problem is performed for verification [14]. Making use of generalized self consistent scheme (GSCS) model, the thermoelastic properties of unidirectional fiber composites with imperfect interface conditions are investigated, and linear relations between interface tractions and displacement jumps are assumed [15]. Linear relation between displacement differences and traction stress across the interface are employed for describing the imperfect interface between fibers and matrix, and the initiation, propagation and arrest of interface cracks of fiber-reinforced composite are analyzed based on a criterion of critical strain energy density [16]. The Mori–Tanaka estimate and its modification are used to evaluate the effective modulus of composites with imperfect interface described by linear spring-layer of vanishing thickness [17]. Making use of conjugate gradient method and fast Fourier transform algorithm, the elastic field and thermal field of two heterogeneous bodies subjected to both contact and frictional heat loads are investigated [18]. Through combining conjugate gradient method and fast Fourier transform methods, a novel method for analyzing the fretting contacts of multilayered or functionally graded materials is proposed, where the frictional contact equations are divided into contact pressure and shear tractions [19]. Similarly, through combining conjugate gradient method (CGM) and the discrete convolution (DC)–fast Fourier transform (FFT) algorithm, efficient semi-analytical solutions are derived for analyzing the resultant electric/magnetic potentials and subsurface stress fields due to 3D frictional magneto-electroelastic (MEE) contact of two multiferroic bodies [20].

Based on the derivation explicit integral kernels for the eigenstrain-induced elastic fields in bi-materials, elastic fields induced by eigenstrains within bimaterials with perfectly bonded and frictionless interfacial conditions are derived [21]. Making use of Chen–Yao's surface elastic theory, size-dependent semi-analytical model (SAM) is proposed for solving the rigid frictionless cylindrical indentation contact of a functionally graded elastic film [22]. Closed-form solutions for the eigenstrain-induced elastic fields in bimaterials with coupled dislocation-like and force-like imperfect interface models are derived [23]. Making use of CGM and FFT, an SAM is developed for treating the surface electric/magnetic potentials and subsurface stresses induced by the frictional MEE surface contact of a multiferroic thin film [24]. Elastic fields caused by pressure and shear tractions applied on the surface of such a layer substrate system are derived based on Papkovich–Neuber potentials, where dislocation-like, force-like, spring-like, and frictionless interfacial conditions are considered [25, 26]. Elastic deformation in bimaterials due to an inclusion with dilatational misfit strain is studied, and dislocation-like interface model is proposed for theoretical explanation [27]. Based on the multi-level multi-summation and conjugate gradient techniques, surface deflections and subsurface stresses for real rough surfaces under contact loading are solved with a single-loop alternative numerical method [28]. A thermo-mechanical model of point contact is established for studying the influence of the size, position and interval of inhomogeneities on temperature field of inhomogeneous materials under frictional heating [29]. Based on the closed-form solution of frequency response functions, coupled thermo-mechanical contact problem of a multilayered material is solved, and resultant heat flux, temperature, displacement and stresses at each interface can be harvested [30]. Making use of closed-form frequency response functions, different kinds of heat flux in multilayered coatings are studied and the resultant thermal fields are derived through thermal conduction equation [31]. Elastic fields of dislocations within isotropic, anisotropic half space, thin film, film-substrate and multilayers systems based on discrete Fourier transformation analysis, where perfect-bounding, linear spring, dislocation-like and force-like interface models are considered, respectively [32–39].

In this paper, an efficient calculation method based on discrete Fourier transformation is developed for evaluating the elastic deformation field of half space, elastic film on elastic substrate, and elastic film on rigid substrate system under known elastic boundary loading conditions. Firstly, the boundary loading is converted to the sum of 2D discrete series through discrete fast Fourier transformation. Then, the elastic fields induced by elastic boundary load is harvested in frequency domain, and the displacement and stress fields continuity are remained for perfectly bounded film substrate system. Given arbitrary distributed boundary stress field at free surface plane of half space and film-substrate system, unique resultant elastic field within the system can be harvested. Afterwards, effects of interface discontinuity are studied, and three types of film-substrate system with imperfect interface models are specially focused: (1) the spring-like imperfect interface model which can be described as: $u_k^f\big|_{z^f=-h} - u_k^s\big|_{z^s=0} = \boldsymbol{K}_T \sigma_{kz}$ and $u_z^f\big|_{z^f=-h} - u_z^s\big|_{z^s=0} = \boldsymbol{K}_N \sigma_{zz}$; (2) the dislocation-like interface model, where interface displacement and stress components relation can be described as: $u_i^f\big|_{z^f=0} = \boldsymbol{k}_{ij}^u\, u_i^s\big|_{z^s=0}$ and $\sigma_{iz}^f\big|_{z^f=0} = \sigma_{iz}^s\big|_{z^s=0}$; (3) the force-like interface model, where interface displacement and stress components relation can be described as: $u_i^f\big|_{z^f=0} = u_i^s\big|_{z^s=0}$ and $\sigma_{iz}^f\big|_{z^f=0} = \boldsymbol{k}_{ij}^t\, \sigma_{iz}^s\big|_{z^s=0}$ respectively. Finally, several simulation examples are performed for verifying the reliability and efficiency of the proposed semi-analytical methods.

Isotropic film-substrate system with perfectly bounded interface conditions is considered, where boundary elastic load is applied on the top surface plane of the film-substrate system, and the film-substrate interface displacement and traction stress components related to film normal direction should be continu-

ous. The mechanical properties of film and substrate materials is isotropic, with modulus and Poisson ratio $(\lambda^f, \mu^f, \upsilon^f)$ and $(\lambda^s, \mu^s, \upsilon^s)$ for the film and substrate, respectively. Based on linear superposition principle of linear elastic problem, the film-substrate system can be divided into two coupled solid regions: thin film and perfectly bounded substrate half space, where the thickness of thin film is $2h$, and $-h \le z^f \le h$ is employed for describing the thin film. Meanwhile, $z^s \le 0$ is employed for describing the substrate, with $z^s = 0$ for the film-substrate interface. The upper symbols "$f$" and "$s$" stand for the film and substrate, $(x^f, y^f)$ and $(x^s, y^s)$ coordinates are employed for describing the in-plane of the film and substrate, respectively. The coordinate origins $(x^f, y^f, z^f)$ for the thin film and $(x^s, y^s, z^s)$ for the substrate are situated at the center of the thin film and the center of the film-substrate interface plane, respectively. As $(x^f, y^f)$ and $(x^s, y^s)$ are identical, they will be written as $(x, y)$ in the following. As shown in Fig. 1, the boundary load $\sigma^f_{iz}|_{\text{load}}$ is applied on the top plane of the thin film, interface displacement and stress components across film-substrate system should satisfy the following elastic field continuity requirements.

(1) Traction stress on top of thin film induced by boundary elastic load should be identical to the resultant elastic stress components within the film-substrate system:

$$\sigma^f_{iz}\big|_{z^f=+h} = \sigma^f_{iz}\big|_{\text{load}}. \tag{1}$$

(2) Resultant elastic displacement and traction stress components across the interface planes of the film-substrate system should be continuous:

$$\sigma^f_{iz}\big|_{z^f=-h} = \sigma^s_{iz}\big|_{z^s=0}, \tag{2}$$

$$u^f_i\big|_{z^f=-h} = u^s_i\big|_{z^s=0}. \tag{3}$$

Normal elastic Hertz load is employed for simulating the elastic deformation of perfectly bounding film-substrate system, the stress distribution in the Hertz load region can be expressed as a function of distance from the center of the Hertz load area [18–20]:

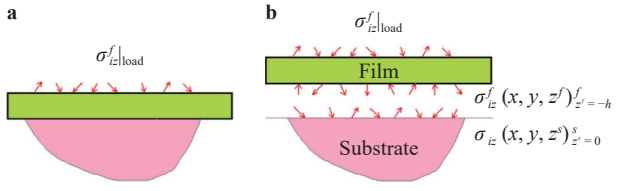


**Fig. 1.** Decomposition of film-substrate system based on linear superposition principle. **a** Elastic load is applied on the top surface plane of the film, and free traction boundary condition should be satisfied on the top surface plane of the film-substrate system. **b** Elastic load stress $\sigma^f_{iz}|_{\text{load}}$ will induce interface traction stress $\sigma_{iz}(x, y, z^f)^f_{z^f=-h}$ on the bottom surface of thin film, and $\sigma_{iz}(x, y, z^s)^s_{z^s=0}$ on the top surface of substrate, continuous interface displacement and interface traction stress are generated across the film-substrate interface plane.

$$|q(r)| = \frac{3P}{2\pi a^2}\sqrt{1-\left(\frac{r}{a}\right)^2}, \tag{4}$$

where $r^2 = x^2 + y^2$, $a$ is the Hertz load patch radius, the maximum pressure $P_0 = 3P/(2\pi a^2)$ is the stress amplitude of the normal contact stress field.

Making use of 2D discrete Fourier transformation, the boundary Hertz load $|q(r)|$ induced traction stress field on the top plane of the film-substrate system can be written in the form of Fourier series:

$$\sigma^f_{iz}(x, y)\big|_{\text{load}} = \sum_{k_x}\sum_{k_y} \widehat{\sigma}^f_{iz}(n_x, n_y)\big|_{\text{load}} \cdot \exp(\mathrm{i}n_x x + \mathrm{i}n_y y). \tag{5}$$

Numerical solutions of Eq. (5) for are considered in the $x$ and $y$ directions with periodic lengths $L_x$ and $L_y$. The wave number is set to be $n_x = 2\pi k_x/L_x$ and $n_y = 2\pi k_y/L_y$, where $k_x = k_y = 0, \pm1, \pm2, \ldots$.

As there is no internal force source and sink, the stress equilibrium equation of the substrate half space can be written as:

$$\mu^s u^s_{i,jj} + (\lambda^s + \mu^s) u^s_{j,ji} = 0, \tag{6}$$

where $u^s_i(x)$ are the displacement components and the elastic constant can be expressed as: $\lambda^s = 2\mu^s\upsilon^s/(1-2\upsilon^s)$, $\mu^s$ and $\upsilon^s$ stand for the shear modulus and Poisson's ratio of substrate medium.

The boundary Hertz elastic load on the top of the film-substrate system will induce stress field within the film-substrate system, resulting in continuous interface traction stress fields $(\sigma^{int}_{iz})$ across the film-substrate interface plane in Cartesian coordinate, which will further generate stress fields within substrate half space medium. Making use of the mathematical completeness of Fourier transformation, the resultant interface elastic field can be written as the sum of Fourier series with unknown Fourier coefficients. The following interface traction stress induced displacement fields are proposed as the solution to Eq. (6), and can be written as:

$$\begin{aligned}
u^s &= \sum_{n_x}\sum_{n_y} \left(+n_x z^s P^s_1 - n_y P^s_2 + \mathrm{i}n_x P^s_3\right) \cdot \exp(n_z z^s) \\
&\quad \cdot \exp(\mathrm{i}kn_x x + \mathrm{i}n_y y), \\
\upsilon^s &= \sum_{n_x}\sum_{n_y} \left(+n_y z^s P^s_1 + n_x P^s_2 + \mathrm{i}n_y P^s_3\right) \cdot \exp(n_z z^s) \\
&\quad \cdot \exp(\mathrm{i}n_x x + \mathrm{i}n_y y), \\
w^s &= \sum_{n_x}\sum_{n_y} \left[\left(-\mathrm{i}n_x z^s + \mathrm{i}\frac{\lambda_s + 3\mu_s}{\lambda_s + \mu_s}\right) P^s_1 + n_z P^s_3\right] \cdot \exp(n_z z^s) \\
&\quad \cdot \exp(\mathrm{i}n_x x + \mathrm{i}n_y y),
\end{aligned} \tag{7}$$

where $n_z = \sqrt{n_x^2 + n_y^2}$, and $(P^s_1, P^s_2, P^s_3)$ are complex constants. The solutions are periodic along $x$ and $y$ directions, and exponential along the $z^s$ direction $(z^s \le 0)$.

Due to the completeness of the Fourier transformation, discrete Fourier coefficient components for certain $(n_x, n_y)$ mode can be written as:

$$\begin{aligned}
\widehat{u}^s &= \left(+n_x z^s P^s_1 - n_y P^s_2 + \mathrm{i}n_x P^s_3\right) \cdot \exp(n_z z^s), \\
\widehat{\upsilon}^s &= \left(+n_y z^s P^s_1 + n_x P^s_2 + \mathrm{i}n_y P^s_3\right) \cdot \exp(n_z z^s), \\
\widehat{w}^s &= \left[\left(-\mathrm{i}n_x z^s + \mathrm{i}\frac{\lambda_s + 3\mu_s}{\lambda_s + \mu_s}\right) P^s_1 + n_z P^s_3\right] \cdot \exp(n_z z^s).
\end{aligned} \tag{8}$$

Thus, the resultant displacement field within substrate half

space is:

$$u_i^s(x,y,z^s)=\sum_{n_x^s}\sum_{n_y^s}\widehat{u}_i^s(n_x,n_y,z^s)\cdot\exp(\mathrm{i}n_x x+\mathrm{i}n_y y). \quad (9)$$

The displacement components $(\widehat{u}^s,\widehat{v}^s,\widehat{w}^s)$ on the interface plane $z^s=0$ for certain $(n_x,n_y)$ mode can be written as:

$$\left\{\begin{array}{c}\widehat{u}^s\\ \widehat{v}^s\\ \widehat{w}^s\end{array}\right\}_{z^s=0}=\boldsymbol{D}^s\cdot\left\{\begin{array}{c}P_1^s\\ P_2^s\\ P_3^s\end{array}\right\}, \quad (10)$$

where the details of $\boldsymbol{D}^s$ are shown in Appendix (A1).

Following the displacement field solution in Eq. (7), it is straightforward to obtain the strain field $\widehat{\varepsilon}_{ij}^s$ through differentiation rule and the resultant stress field $\widehat{\sigma}_{ij}^s$ on the top plane $z^s=0$ of the film-substrate system.

The interface stress components on the film-substrate interface plane $z^s=0$ for certain $(n_x,n_y)$ mode can be written as:

$$\left\{\begin{array}{c}\widehat{\sigma}_{xz}^S\\ \widehat{\sigma}_{yz}^S\\ \widehat{\sigma}_{zz}^S\end{array}\right\}_{z^s=0}=\boldsymbol{T}^s\cdot\left\{\begin{array}{c}P_1^s\\ P_2^s\\ P_3^s\end{array}\right\}\cdot\exp(\mathrm{i}n_x x+\mathrm{i}n_y y), \quad (11)$$

and the details of $\boldsymbol{T}^s$ are shown in Appendix (A2).

Numerical solutions of Eqs. (7)-(11) for the substrate medium are considered in the $x$ and $y$ directions with periodic lengths $L_x$ and $L_y$. The wave number is set to be $n_x=2\pi k_x/L_x$ and $n_y=2\pi k_y/L_y$, where $k_x=k_y=0,\pm1,\pm2,\ldots$.

Similar to the above elastic boundary load induced deformation of half space, an arbitrary displacement field induced by elastic Hertz load on the upper surface plane of thin film can be written in the form of Fourier series with unknown Fourier coefficients. As there is no internal bulk force source and sink, the stress equilibrium equation of the thin film can be written in terms of displacement components $u_i^f(x)$:

$$\mu^f u_{i,jj}^f+(\lambda^f+\mu^f)u_{j,ji}^f=0, \quad (12)$$

where $\lambda^f=2\mu^f\nu^f/(1-2\nu^f)$, $\mu^f$ and $\nu^f$ are the shear modulus and Poisson's ratio for the thin film medium, which is assumed to have a thickness of $2h$ in the $z^f$ direction, and $-h\le z^f\le h$.

The elastic field can be written as sum of Fourier series, and the solution is periodic in the $x$ and $y$ directions, and hyperbolic in the $z^f$ direction, with the coordinate origin situated at the middle center of the thin film:

$$\begin{aligned}u^f&=\sum_{n_x}\sum_{n_y}\left[\begin{array}{c}(n_x z^f A-n_y F+\mathrm{i}n_x G)\sinh(n_z z^f)\\ +(n_x z^f E+n_y B+\mathrm{i}n_x C)\cosh(n_z z^f)\end{array}\right]\\ &\quad\cdot\exp(\mathrm{i}n_x x+\mathrm{i}n_y y),\\ v^f&=\sum_{n_x}\sum_{n_y}\left[\begin{array}{c}(n_y z^f A+n_x F+\mathrm{i}n_y G)\sinh(n_z z^f)\\ +(n_y z^f E-n_x B+\mathrm{i}n_y C)\cosh(n_z z^f)\end{array}\right]\\ &\quad\cdot\exp(\mathrm{i}n_x x+\mathrm{i}n_y y),\\ w^f&=\sum_{n_x}\sum_{n_y}\left[\begin{array}{c}\left(-\mathrm{i}n_z z^f A+\mathrm{i}\dfrac{\lambda_f+3\mu_f}{\lambda_f+\mu_f}E+n_z G\right)\cosh(n_z z^f)\\ +\left(-\mathrm{i}n_z z^f E+\mathrm{i}\dfrac{\lambda_f+3\mu_f}{\lambda_f+\mu_f}A+n_z C\right)\sinh(n_z z^f)\end{array}\right]\\ &\quad\cdot\exp(\mathrm{i}n_x x+\mathrm{i}n_y y),\end{aligned} \quad (13)$$

where $n_z=\sqrt{n_x^2+n_y^2}$, and the unknown terms $(A,B,C)$ and $(E,F,G)$ are complex constants.

Due to the mathematical completeness of Fourier series, the Fourier coefficient components for each Fourier $(n_x,n_y)$ mode is:

$$\begin{aligned}\widehat{u}^f&=(n_x z^f A-n_y F+\mathrm{i}n_x G)\sinh(n_z z^f)+(n_x z^f E+n_y B+\mathrm{i}n_x C)\\ &\quad\cdot\cosh(n_z z^f),\\ \widehat{v}^f&=(n_y z^f A+n_x F+\mathrm{i}n_y G)\sinh(n_z z^f)+(n_y z^f E-n_x B+\mathrm{i}n_y C)\\ &\quad\cdot\cosh(n_z z^f),\\ \widehat{w}^f&=\left(-\mathrm{i}n_z z^f A+\mathrm{i}\frac{\lambda_f+3\mu_f}{\lambda_f+\mu_f}E+n_z G\right)\cosh(n_z z^f)\\ &\quad+\left(-\mathrm{i}n_z z^f E+\mathrm{i}\frac{\lambda_f+3\mu_f}{\lambda_f+\mu_f}A+n_z C\right)\sinh(n_z z^f).\end{aligned} \quad (14)$$

Alternatively, the elastic displacement components within thin film in Eq. (13) can be written as:

$$u_i^f(x,y,z^f)=\sum_{n_x}\sum_{n_y}\widehat{u}_i^f(n_x,n_y,z^f)\cdot\exp(\mathrm{i}n_x x+\mathrm{i}n_y y), \quad (15)$$

and the resultant stress components can be obtained from isotropic Hooke's law:

$$\sigma_{iz}^f(x,y,z^f)=\sum_{n_x}\sum_{n_y}\widehat{\sigma}_{iz}^f(n_x,n_y,z^f)\cdot\exp(\mathrm{i}n_x x+\mathrm{i}n_y y). \quad (16)$$

When $z^f=\pm h$, the stress components are elastic contact stress components at the upper surface, and the interface stress components of the film-substrate system.

Then, Eq. (15) was submitted into Eq. (12), resultant displacement fields on the top surface and film-substrate interface planes $z^f=\pm h$ can be combined together, and rewritten into two sets of equations on unknown coefficients $(A,B,C)$ and $(E,F,G)$, which correspond to the symmetrical and the asymmetrical displacement parts, respectively.

The symmetrical correction displacement is:

$$\begin{aligned}\boldsymbol{u}^{\mathrm{syym}}&=\frac{1}{2}\left[\begin{array}{c}\widehat{u}^f\big|_{z^f=+h}+\widehat{u}^f\big|_{z^f=-h}\\ \widehat{v}^f\big|_{z^f=+h}+\widehat{v}^f\big|_{z^f=-h}\\ \widehat{w}^f\big|_{z^f=+h}-\widehat{w}^f\big|_{z^f=-h}\end{array}\right]=\boldsymbol{D}^{\mathrm{syym}}\cdot\left\{\begin{array}{c}A\\ B\\ C\end{array}\right\}\\ &\quad\cdot\exp(\mathrm{i}n_x x+\mathrm{i}n_y y),\end{aligned} \quad (17)$$

and the asymmetrical correction displacement part is:

$$\begin{aligned}\boldsymbol{u}^{\mathrm{assym}}&=\frac{1}{2}\left[\begin{array}{c}\widehat{u}^f\big|_{z^f=+h}-\widehat{u}^f\big|_{z^f=-h}\\ \widehat{v}^f\big|_{z^f=+h}-\widehat{v}^f\big|_{z^f=-h}\\ \widehat{w}^f\big|_{z^f=+h}+\widehat{w}^f\big|_{z^f=-h}\end{array}\right]=\boldsymbol{D}^{\mathrm{assym}}\cdot\left\{\begin{array}{c}E\\ F\\ G\end{array}\right\}\\ &\quad\cdot\exp(\mathrm{i}n_x x+\mathrm{i}n_y y).\end{aligned} \quad (18)$$

The symmetrical stress is:

$$\begin{aligned}\boldsymbol{\sigma}^{\mathrm{syym}}&=\frac{1}{2}\left[\begin{array}{c}\sigma_{xz}^f\big|_{z^f=+h}-\sigma_{xz}^f\big|_{z^f=-h}\\ \sigma_{yz}^f\big|_{z^f=+h}-\sigma_{yz}^f\big|_{z^f=-h}\\ \sigma_{zz}^f\big|_{z^f=+h}+\sigma_{zz}^f\big|_{z^f=-h}\end{array}\right]=\boldsymbol{T}^{\mathrm{syym}}\cdot\left\{\begin{array}{c}A\\ B\\ C\end{array}\right\}\\ &\quad\cdot\exp(\mathrm{i}n_x x+\mathrm{i}n_y y),\end{aligned} \quad (19)$$

and the asymmetrical stress is:

$$\boldsymbol{\sigma}^{\text{assym}} = \frac{1}{2}\begin{bmatrix} \sigma^f_{xz}\big|_{z^f=+h} + \sigma^f_{xz}\big|_{z^f=-h} \\ \sigma^f_{yz}\big|_{z^f=+h} + \sigma^f_{yz}\big|_{z^f=-h} \\ \sigma^f_{zz}\big|_{z^f=+h} - \sigma^f_{zz}\big|_{z^f=-h} \end{bmatrix} = \boldsymbol{T}^{\text{assym}} \cdot \begin{Bmatrix} E \\ F \\ G \end{Bmatrix} \cdot \exp\left(\mathrm{i}n_x x + \mathrm{i}n_y y\right). \tag{20}$$

The details of $\boldsymbol{D}^{\text{syym}}$, $\boldsymbol{D}^{\text{assym}}$, $\boldsymbol{T}^{\text{syym}}$ and $\boldsymbol{T}^{\text{assym}}$ for thin film are given in Appendix (A3)-(A6).

Similar to the calculation procedures for the substrate half space, numerical simulations of Eqs. (12)-(20) for isotropic thin film of the film-substrate system are considered in the $x$ and $y$ directions with periodic lengths $L_x$ and $L_y$. The wave number is set to be $n_x = 2\pi k_x / L_x$ and $n_y = 2\pi k_y / L_y$, where $k_x = k_y = 0, \pm1, \pm2, \ldots$.

Considering the interface displacement and traction stress continuity requirements for the perfect bonding film-substrate system under elastic contact loading, following relation should be satisfied for each $(n_x, n_y)$ Fourier mode.

Through the comparison between Eqs. (5) and (16), elastic Hertz boundary load stress on the top plane of the perfect bonding film-substrate system should be satisfied the following equation:

$$\sigma^f_{iz}\left(x, y, z^f\right)_{z^f=+h} = \sigma^f_{iz}\big|_{\text{load}}. \tag{21}$$

Interface traction stress and displacement continuity across the interface plane of the perfect bonding film-substrate system should be satisfied:

$$\sigma_{iz}\left(x, y, z^f\right)^f_{z^f=-h} = \sigma_{iz}\left(x, y, z^s\right)^s_{z^s=0}, \tag{22}$$

$$u_i\left(x, y, z^f\right)^f_{z^f=-h} = u_i\left(x, y, z^s\right)^s_{z^s=0}. \tag{23}$$

After submitting the boundary Hertz load in Eq. (5), resultant elastic fields in Eqs. (10) and (11) for substrate and Eqs. (17)-(20) for thin film into Eqs. (21)-(23) for film-substrate system, the following relations stand for each $(n_x, n_y)$ Fourier mode.

(1) Elastic contact stress equilibrium should be satisfied on the top surface plane of the thin filmfor each $(n_x, n_y)$ Fourier mode:

$$\boldsymbol{T}^{\text{syym}}\begin{Bmatrix} A \\ B \\ C \end{Bmatrix} + \boldsymbol{T}^{\text{assym}}\begin{Bmatrix} E \\ F \\ G \end{Bmatrix} = \begin{bmatrix} \widehat{\sigma}^f_{xz}\big|_{\text{load}} \\ \widehat{\sigma}^f_{yz}\big|_{\text{load}} \\ \widehat{\sigma}^f_{zz}\big|_{\text{load}} \end{bmatrix}. \tag{24}$$

(2) Interface traction stress should be continuous for each $(n_x, n_y)$ Fourier mode:

$$\boldsymbol{K}_{ij} \cdot \left[-\boldsymbol{T}^{\text{syym}}\begin{Bmatrix} A \\ B \\ C \end{Bmatrix} + \boldsymbol{T}^{\text{assym}}\begin{Bmatrix} E \\ F \\ G \end{Bmatrix}\right] = \boldsymbol{T}^s \begin{Bmatrix} P^s_1 \\ P^s_2 \\ P^s_3 \end{Bmatrix}, \tag{25}$$

in which $\boldsymbol{K}_{ij} = \text{diag}\{1, 1, -1\}$ is a 3×3 diagonal matrix.

(3) Interface displacement should be continuous for each $(n_x, n_y)$ Fourier mode:

$$\boldsymbol{K}_{ij} \cdot \left[\boldsymbol{D}^{\text{syym}}\begin{Bmatrix} A \\ B \\ C \end{Bmatrix} - \boldsymbol{D}^{\text{assym}}\begin{Bmatrix} E \\ F \\ G \end{Bmatrix}\right] = \boldsymbol{D}^s \begin{Bmatrix} P^s_1 \\ P^s_2 \\ P^s_3 \end{Bmatrix}. \tag{26}$$

In summary, Eqs. (24)-(26) can be written together as:

$$\begin{bmatrix} \boldsymbol{T}^{\text{syym}} & \boldsymbol{T}^{\text{assym}} & 0 \\ -\boldsymbol{K}_{ij} \cdot \boldsymbol{T}^{\text{syym}} & \boldsymbol{K}_{ij} \cdot \boldsymbol{T}^{\text{assym}} & -\boldsymbol{T}^s \\ \boldsymbol{K}_{ij} \cdot \boldsymbol{D}^{\text{syym}} & -\boldsymbol{K}_{ij} \cdot \boldsymbol{D}^{\text{assym}} & -\boldsymbol{D}^s \end{bmatrix} \cdot \begin{Bmatrix} A \\ B \\ C \\ E \\ F \\ G \\ P^s_1 \\ P^s_2 \\ P^s_3 \end{Bmatrix} = \begin{Bmatrix} \widehat{\sigma}^f_{xz}\big|_{\text{load}} \\ \widehat{\sigma}^f_{yz}\big|_{\text{load}} \\ \widehat{\sigma}^f_{zz}\big|_{\text{load}} \\ 0 \\ 0 \\ 0 \\ 0 \\ 0 \\ 0 \end{Bmatrix}. \tag{27}$$

Then, unknown coefficient $(A, B, C, E, F, G)$ and $\left(P^s_1, P^s_2, P^s_3\right)$ of thin film and substrate displacement can be solved from Eq. (27), and the resultant elastic field within the film medium and substrate medium can be generated.

As to film on rigid substrate special case, zero displacement requirements at the interface plane of perfect bonding film-substrate system should be satisfied, and following relation stands for each $(n_x, n_y)$ Fourier mode.

Elastic contact stress on the top plane of the perfect bonding film-substrate system should be satisfied:

$$\{\widehat{\sigma}_{iz}\}^f_{z^f=+h} = \sigma^f_{iz}\big|_{\text{load}}. \tag{28}$$

Interface displacement continuity and zero displacement restrictions across the interface plane of the perfect bonding film-substrate system should be satisfied:

$$\{\widehat{u}_i\}^f_{z^f=-h} = \{\widehat{u}_i\}^s_{z^s=0} = 0. \tag{29}$$

After submitting boundary Hertz load Eq. (5), the resultant elastic fields Eqs. (10) and (11) for substrate and Eqs. (17)-(20) for thin film into Eqs. (28) and (29), the following relations should be satisfied for each $(n_x, n_y)$ Fourier mode.

(1) Elastic contact boundary condition should be satisfied on the top surface plane of the thin film for each $(n_x, n_y)$ Fourier mode:

$$\boldsymbol{T}^{\text{syym}}\begin{Bmatrix} A \\ B \\ C \end{Bmatrix} + \boldsymbol{T}^{\text{assym}}\begin{Bmatrix} E \\ F \\ G \end{Bmatrix} = \begin{bmatrix} \widehat{\sigma}^f_{xz}\big|_{\text{load}} \\ \widehat{\sigma}^f_{yz}\big|_{\text{load}} \\ \widehat{\sigma}^f_{zz}\big|_{\text{load}} \end{bmatrix}. \tag{30}$$

(2) Interface displacement should be zero for each $(n_x, n_y)$ Fourier mode:

$$\boldsymbol{K}_{ij} \cdot \left[\boldsymbol{D}^{\text{syym}}\begin{Bmatrix} A \\ B \\ C \end{Bmatrix} - \boldsymbol{D}^{\text{assym}}\begin{Bmatrix} E \\ F \\ G \end{Bmatrix}\right] = 0. \tag{31}$$

In summary, Eqs. (30) and (31) can be written together as:

$$\begin{bmatrix} \boldsymbol{T}^{\text{syym}} & \boldsymbol{T}^{\text{assym}} \\ -\boldsymbol{K}_{ij}\cdot\boldsymbol{T}^{\text{syym}} & \boldsymbol{K}_{ij}\cdot\boldsymbol{T}^{\text{assym}} \end{bmatrix} \cdot \begin{Bmatrix} A \\ B \\ C \\ E \\ F \\ G \end{Bmatrix} = \begin{Bmatrix} \widehat{\sigma}^{f}_{xz}\big|_{\text{load}} \\ \widehat{\sigma}^{f}_{yz}\big|_{\text{load}} \\ \widehat{\sigma}^{f}_{zz}\big|_{\text{load}} \\ 0 \\ 0 \\ 0 \end{Bmatrix}. \tag{32}$$

Then, unknown coefficient $(A,B,C,E,F,G)$ can be solved from Eq. (32), and the resultant elastic field within the film medium can be generated.

When considering the problem of isotropic film-substrate system with linear spring-like imperfect interface conditions, the elastic field on the interface plane will be modified due to the stiffness mismatch and interface imperfection. In this linear spring-like model, the interfacial tractions become continuous, the displacements across the interface plane are discontinuous, and the displacement jump is linearly proportional to interfacial traction stress components:

$$u^{f}_{k}\big|_{z^f=-h} - u^{s}_{k}\big|_{z^s=0} = \boldsymbol{K}_T\sigma_{kz}, \quad k=1,2, \tag{33}$$

$$u^{f}_{z}\big|_{z^f=-h} - u^{s}_{z}\big|_{z^s=0} = \boldsymbol{K}_N\sigma_{zz}, \tag{34}$$

$$\sigma^{f}_{iz}\big|_{z^f=-h} = \sigma^{s}_{iz}\big|_{z^s=0}, \tag{35}$$

in which, the linear-spring interface related matrixes $\boldsymbol{K}_T$ and $\boldsymbol{K}_N$ are constant, demonstrating that the interface traction stress is continuous, while the displacement jump across the interface is related to the interface shearing and normal stress components.

Finally, according to the linear spring-like interface model in Eqs. (33)–(35), the displacement and traction stress across the film-substrate interface plane should satisfy:

(1) elastic contact stress on the top plane of the perfect bonding film-substrate system should be satisfied:

$$\widehat{\sigma}_{iz}\left(x,y,z^f\right)^{f}_{z^f=+h} = \widehat{\sigma}^{f}_{iz}\big|_{\text{load}}; \tag{36}$$

(2) interface traction stress continuity and displacement jump across the interface plane of the linear spring-like film-substrate system should be satisfied:

$$\widehat{u}_i\left(x,y,z^f\right)^{f}_{z^f=-h} = \widehat{u}_i\left(x,y,z^s\right)^{s}_{z^s=0} + \boldsymbol{K}^t\cdot\widehat{\sigma}_{iz}\left(x,y,z^s\right)^{s}_{z^s=0}, \quad i=1,2, \tag{37}$$

$$\widehat{u}_i\left(x,y,z^f\right)^{f}_{z^f=-h} = \boldsymbol{K}^N\cdot\widehat{u}_i\left(x,y,z^s\right)^{s}_{z^s=0}, \tag{38}$$

$$\widehat{\sigma}_{iz}\left(x,y,z^f\right)^{f}_{z^f=-h} = \widehat{\sigma}_{iz}\left(x,y,z^s\right)^{s}_{z^s=0}, \quad i=1,2. \tag{39}$$

After submitting boundary Hertz load Eq. (5), the resultant elastic fields Eqs. (10) and (11) for substrate and Eqs. (17)–(20) for thin film into Eqs. (36)–(39), the following relations stand for each $(n_x,n_y)$ Fourier mode.

(1) Elastic contact boundary condition should be satisfied on the top surface plane of the thin film for each $(n_x,n_y)$ Fourier mode:

$$\boldsymbol{T}^{\text{syym}}\begin{Bmatrix} A \\ B \\ C \end{Bmatrix} + \boldsymbol{T}^{\text{assym}}\begin{Bmatrix} E \\ F \\ G \end{Bmatrix} = \begin{bmatrix} \widehat{\sigma}^{f}_{xz}\big|_{\text{load}} \\ \widehat{\sigma}^{f}_{yz}\big|_{\text{load}} \\ \widehat{\sigma}^{f}_{zz}\big|_{\text{load}} \end{bmatrix}. \tag{40}$$

(2) Interface traction stress should be continuous for each $(n_x,n_y)$ Fourier mode:

$$\boldsymbol{K}_{ij}\cdot\left[-\boldsymbol{T}^{\text{syym}}\begin{Bmatrix} A \\ B \\ C \end{Bmatrix} + \boldsymbol{T}^{\text{assym}}\begin{Bmatrix} E \\ F \\ G \end{Bmatrix}\right] = \boldsymbol{T}^{s}\begin{Bmatrix} P^s_1 \\ P^s_2 \\ P^s_3 \end{Bmatrix}, \tag{41}$$

in which, $\boldsymbol{K}_{ij}=\text{diag}\{1,1,-1\}$ is a 3×3 diagonal matrix, and the constant matrix.

(3) Interface displacement jump should satisfy the following linear-spring displacement-stress relations for each $(n_x,n_y)$ Fourier mode:

$$\begin{aligned}\boldsymbol{K}_{ij}\cdot\left[\boldsymbol{D}^{\text{syym}}\begin{Bmatrix} A \\ B \\ C \end{Bmatrix} - \boldsymbol{D}^{\text{assym}}\begin{Bmatrix} E \\ F \\ G \end{Bmatrix}\right] \\ = \boldsymbol{D}^{s}\begin{Bmatrix} P^s_1 \\ P^s_2 \\ P^s_3 \end{Bmatrix} + \boldsymbol{K}^{s}\cdot\boldsymbol{T}^{s}\begin{Bmatrix} P^s_1 \\ P^s_2 \\ P^s_3 \end{Bmatrix}.\end{aligned} \tag{42}$$

In summary, Eqs. (40)–(42) can be written together as:

$$\begin{bmatrix} \boldsymbol{T}^{\text{syym}} & \boldsymbol{T}^{\text{assym}} & 0 \\ -\boldsymbol{K}_{ij}\cdot\boldsymbol{T}^{\text{assym}} & \boldsymbol{K}_{ij}\cdot\boldsymbol{T}^{\text{assym}} & -\boldsymbol{T}^{s} \\ \boldsymbol{K}_{ij}\cdot\boldsymbol{D}^{\text{syym}} & -\boldsymbol{K}_{ij}\cdot\boldsymbol{D}^{\text{assym}} & -\boldsymbol{D}^{s}-\boldsymbol{K}^{s}\cdot\boldsymbol{T}^{s} \end{bmatrix} \cdot \begin{Bmatrix} A \\ B \\ C \\ E \\ F \\ G \\ P^s_1 \\ P^s_2 \\ P^s_3 \end{Bmatrix} = \begin{Bmatrix} \widehat{\sigma}^{f}_{xz}\big|_{\text{load}} \\ \widehat{\sigma}^{f}_{yz}\big|_{\text{load}} \\ \widehat{\sigma}^{f}_{zz}\big|_{\text{load}} \\ 0 \\ 0 \\ 0 \\ 0 \\ 0 \\ 0 \end{Bmatrix}. \tag{43}$$

Then, unknown coefficient $(A,B,C,E,F,G)$ and $\left(P^s_1,P^s_2,P^s_3\right)$ of correction displacement can be solved from Eq. (43), and the resultant elastic field within the film medium and substrate medium can be generated.

In this dislocation-like imperfect interface model, the traction stress is continuous while the displacement is discontinuous across the interface plane:

$$u^{f}_{i}\big|_{z^f=-h} = \boldsymbol{k}^{u}_{ij}\,u^{s}_{i}\big|_{z^s=0}, \tag{44}$$

$$\sigma_{iz}^{f}\big|_{z^f=-h} = \sigma_{iz}^{s}\big|_{z^s=0}, \tag{45}$$

where the constant matrix $\boldsymbol{K}^u = \boldsymbol{k}_{ij}^u$ describes the bonding condition at the interface plane of dislocation-like interface model. The constant matrix $\boldsymbol{k}_{ij}^u$ is diagonal, where the first two elements on the diagonal are related to the interface conditions in the tangential directions and the third one to the condition in the normal direction of the interface.

Finally, according to the dislocation-like interface model in Eqs. (44) and (45), the displacement and traction stress across the interface plane of film-substrate system should satisfy the following conditions for each $(n_x, n_y)$ Fourier mode.

Elastic contact stress on the top plane of the film-substrate system with dislocation-like interface condition should satisfy:

$$\widehat{\sigma}_{iz}\left(x, y, z^f\right)_{z^f=+h}^{f} = \widehat{\sigma}_{iz}^{f}\big|_{\text{load}}. \tag{46}$$

Interface traction stress continuity and interface displacement jump across the interface plane of the film-substrate system with dislocation-like interface condition should satisfy:

$$\widehat{\sigma}_{iz}\left(x, y, z^f\right)_{z^f=-h}^{f} = \widehat{\sigma}_{iz}\left(x, y, z^s\right)_{z^s=0}^{s}, \tag{47}$$

$$\widehat{u}_i\left(x, y, z^f\right)_{z^f=-h}^{f} = \boldsymbol{K}^u \cdot \widehat{u}_i\left(x, y, z^s\right)_{z^s=0}^{s}. \tag{48}$$

After submitting boundary Hertz load Eq. (5), the resultant elastic fields Eqs. (10) and (11) for substrate and Eqs. (17)–(20) for thin film into Eqs. (46)–(48), the following relations stand for each $(n_x, n_y)$ Fourier mode.

(1) Elastic contact boundary condition should be satisfied on the top surface plane of the thin film for each $(n_x, n_y)$ Fourier mode:

$$\boldsymbol{T}^{\text{syym}} \begin{Bmatrix} A \\ B \\ C \end{Bmatrix} + \boldsymbol{T}^{\text{assym}} \begin{Bmatrix} E \\ F \\ G \end{Bmatrix} = \begin{bmatrix} \widehat{\sigma}_{xz}^{f}\big|_{\text{load}} \\ \widehat{\sigma}_{yz}^{f}\big|_{\text{load}} \\ \widehat{\sigma}_{zz}^{f}\big|_{\text{load}} \end{bmatrix}. \tag{49}$$

(2) Interface traction stress should be continuous for each $(n_x, n_y)$ Fourier mode:

$$\boldsymbol{K}_{ij} \cdot \left[ -\boldsymbol{T}^{\text{syym}} \begin{Bmatrix} A \\ B \\ C \end{Bmatrix} + \boldsymbol{T}^{\text{assym}} \begin{Bmatrix} E \\ F \\ G \end{Bmatrix} \right] = \boldsymbol{T}^{s} \begin{Bmatrix} P_1^s \\ P_2^s \\ P_3^s \end{Bmatrix}, \tag{50}$$

in which, $\boldsymbol{K}_{ij} = \text{diag}\{1, 1, -1\}$ is a 3×3 diagonal matrix.

(3) Interface displacement jump across the interface plane should satisfy the following relation for each $(n_x, n_y)$ Fourier mode:

$$\boldsymbol{K}_{ij} \cdot \left[ \boldsymbol{D}^{\text{syym}} \begin{Bmatrix} A \\ B \\ C \end{Bmatrix} - \boldsymbol{D}^{\text{assym}} \begin{Bmatrix} E \\ F \\ G \end{Bmatrix} \right] = \boldsymbol{K}^u \cdot \boldsymbol{D}^{s} \begin{Bmatrix} P_1^s \\ P_2^s \\ P_3^s \end{Bmatrix}. \tag{51}$$

In summary, Eqs. (49)–(51) can be written together as:

$$\begin{bmatrix} \boldsymbol{T}^{\text{syym}} & \boldsymbol{T}^{\text{assym}} & 0 \\ -\boldsymbol{K}_{ij} \cdot \boldsymbol{T}^{\text{syym}} & \boldsymbol{K}_{ij} \cdot \boldsymbol{T}^{\text{assym}} & -\boldsymbol{T}^{s} \\ \boldsymbol{K}_{ij} \cdot \boldsymbol{D}^{\text{syym}} & -\boldsymbol{K}_{ij} \cdot \boldsymbol{D}^{\text{assym}} & -\boldsymbol{K}^u \cdot \boldsymbol{D}^{s} \end{bmatrix} \cdot \begin{Bmatrix} A \\ B \\ C \\ E \\ F \\ G \\ P_1^s \\ P_2^s \\ P_3^s \end{Bmatrix} = \begin{Bmatrix} \widehat{\sigma}_{xz}^{f}\big|_{\text{load}} \\ \widehat{\sigma}_{yz}^{f}\big|_{\text{load}} \\ \widehat{\sigma}_{zz}^{f}\big|_{\text{load}} \\ 0 \\ 0 \\ 0 \\ 0 \\ 0 \\ 0 \end{Bmatrix}. \tag{52}$$

Then, unknown coefficient $(A, B, C, E, F, G)$ and $\left(P_1^s, P_2^s, P_3^s\right)$ of resultant displacement can be solved from Eq. (52), and the resultant elastic field within the film medium and substrate medium can be generated.

In force-like imperfect interface model, the displacement vector is continuous while the traction stress vector is discontinuous across the interface of the film-substrate system:

$$u_i^f\big|_{z^f=-h} = u_i^s\big|_{z^s=0}, \tag{53}$$

$$\sigma_{iz}^{f}\big|_{z^f=-h} = \boldsymbol{k}_{ij}^t\, \sigma_{iz}^{s}\big|_{z^s=0}, \tag{54}$$

where the constant matrix $\boldsymbol{K}^t = \boldsymbol{k}_{ij}^t$ describes the bonding condition at the interface plane. Similar to the dislocation-like model, if the constant matrix $\boldsymbol{k}_{ij}^t$ is diagonal, then the first two elements on the diagonal are related to the interface conditions in the tangential directions and the third one to the condition in the normal direction of the interface.

Finally, according to the force-like interface model in Eqs. (53) and (54), the displacement and traction stress across the film-substrate interface plane should satisfy the following relation stands for each $(n_x, n_y)$ Fourier mode.

(1) Elastic contact stress on the top plane of the perfect bonding film-substrate system should be satisfied:

$$\widehat{\sigma}_{iz}\left(x, y, z^f\right)_{z^f=+h}^{f} = \widehat{\sigma}_{iz}^{f}\big|_{\text{load}}. \tag{55}$$

(2) Interface displacement continuity and traction stress discontinuity across the interface plane of the film-substrate system should be satisfied:

$$\widehat{\sigma}_{iz}\left(x, y, z^f\right)_{z^f=-h}^{f} = \boldsymbol{K}^t \cdot \widehat{\sigma}_{iz}\left(x, y, z^s\right)_{z^s=0}^{s}, \tag{56}$$

$$\widehat{u}_i\left(x, y, z^f\right)_{z^f=-h}^{f} = \widehat{u}_i\left(x, y, z^s\right)_{z^s=0}^{s}. \tag{57}$$

After submitting boundary Hertz load Eq. (5), the resultant elastic fields Eqs. (10) and (11) for substrate and Eqs. (17)–(20) for thin film into Eqs. (56) and (57), the following relations stand for each $(n_x, n_y)$ Fourier mode.

(1) Elastic contact boundary condition should be satisfied on the top surface plane of the thin film for each $(n_x, n_y)$ Fourier mode:

$$\boldsymbol{T}^{\text{syym}}\begin{Bmatrix} A \\ B \\ C \end{Bmatrix} + \boldsymbol{T}^{\text{assym}}\begin{Bmatrix} E \\ F \\ G \end{Bmatrix} = \begin{bmatrix} \widehat{\sigma}^f_{xz}\big|_{\text{load}} \\ \widehat{\sigma}^f_{yz}\big|_{\text{load}} \\ \widehat{\sigma}^f_{zz}\big|_{\text{load}} \end{bmatrix}. \tag{58}$$

(2) Interface traction stress should satisfy the following relation for each $(n_x, n_y)$ Fourier mode:

$$\boldsymbol{K}_{ij}\cdot\left[-\boldsymbol{T}^{\text{syym}}\begin{Bmatrix} A \\ B \\ C \end{Bmatrix} + \boldsymbol{T}^{\text{assym}}\begin{Bmatrix} E \\ F \\ G \end{Bmatrix}\right] = \boldsymbol{K}^t\cdot\boldsymbol{T}^s\begin{Bmatrix} P^s_1 \\ P^s_2 \\ P^s_3 \end{Bmatrix}, \tag{59}$$

in which, $\boldsymbol{K}_{ij} = \text{diag}\{1, 1, -1\}$ is a 3×3 diagonal matrix, and the constant matrix $\boldsymbol{K}^t = \boldsymbol{k}^t_{ij}$ describes the bonding condition at the interface plane.

(3) Interface displacement should be continuous for each $(n_x, n_y)$ Fourier mode:

$$\boldsymbol{K}_{ij}\cdot\left[\boldsymbol{D}^{\text{syym}}\begin{Bmatrix} A \\ B \\ C \end{Bmatrix} - \boldsymbol{D}^{\text{assym}}\begin{Bmatrix} E \\ F \\ G \end{Bmatrix}\right] = \boldsymbol{D}^s\begin{Bmatrix} P^s_1 \\ P^s_2 \\ P^s_3 \end{Bmatrix}. \tag{60}$$

In summary, Eqs. (58)–(60) can be written together as:

$$\begin{bmatrix} \boldsymbol{T}^{\text{syym}} & \boldsymbol{T}^{\text{assym}} & 0 \\ -\boldsymbol{K}_{ij}\cdot\boldsymbol{T}^{\text{syym}} & \boldsymbol{K}_{ij}\cdot\boldsymbol{T}^{\text{assym}} & -\boldsymbol{K}^t\cdot\boldsymbol{T}^s \\ \boldsymbol{K}_{ij}\cdot\boldsymbol{D}^{\text{syym}} & -\boldsymbol{K}_{ij}\cdot\boldsymbol{D}^{\text{assym}} & -\boldsymbol{D}^s \end{bmatrix} \cdot \begin{Bmatrix} A \\ B \\ C \\ E \\ F \\ G \\ P^s_1 \\ P^s_2 \\ P^s_3 \end{Bmatrix} = \begin{Bmatrix} \widehat{\sigma}^f_{xz}\big|_{\text{load}} \\ \widehat{\sigma}^f_{yz}\big|_{\text{load}} \\ \widehat{\sigma}^f_{zz}\big|_{\text{load}} \\ 0 \\ 0 \\ 0 \\ 0 \\ 0 \\ 0 \end{Bmatrix}. \tag{61}$$

Then, unknown coefficient $(A, B, C, E, F, G)$ and $(P^s_1, P^s_2, P^s_3)$ of correction displacement can be solved from Eq. (61), and the resultant elastic field within the film medium and substrate medium can be generated.

In the following, Hertz elastic boundary load on isotropic Cu-Nb film-substrate system is investigated. The elastic modulus of Cu and Nb is shown in Table 1 [40], and the isotropic equivalent shear modulus and Poisson's ratio are treated with Voigt isotropic model [41].

The elastic Hertz boundary load on the top surface plane of half space is assumed, as described by Eq. (4), the contact radius is $a = 5$ nm, and Hertz stress amplitude $P_0 = 5$ GPa. The material of half space is Nb, with its Voigt isotropic modulus shown in Table. 1. The stress field within the cross-section of half space is plotted with physical scale along $x$ direction $L_x = 60$ nm and physical scale along $z$ direction $z_0 = 40$ nm, and the periodic Fourier transformation wave number is: $n_x = n_y = 30$. The produced stress fields under normal Hertz boundary load are: Fig. 2a for $\sigma_{xz}$, Fig. 2b for $\sigma_{zz}$, Fig. 2c for $u_x$ and Fig. 2d for $u_z$, respectively.

Hertz load acting on top surface plane of isotropic elastic film-substrate system is simulated, as described by Eq. (4), where the contact radius $a = 5$ nm, and Hertz stress amplitude $P_0 = 5$ GPa. The material of thin film is Cu and the substrate is Nb, with their Voigt isotropic modulus shown in Table 1. The geometrical parameters of thin film are: thickness: $h$=20 mm, the stress field within the cross-section of film-substrate system is plotted with physical scale along $x$ direction $L_x = 60$ nm and physical scale along $z$ direction $z_0 = 60$ nm, including 20 nm thin film and 40 nm substrate along z direction. The periodic Fourier transformation wave number is $k_x = k_y = 30$. The produced stress fields under normal traction Hertz load are: Fig. 3a for $\sigma_{xz}$, Fig. 3b for $\sigma_{zz}$, Fig. 3c for $u_x$and Fig. 3d for $u_z$, respectively. Comparisons of interface traction and displacement profiles along $x$ direction in the $xz$ plane ($y$=0) are shown in Fig. 4. Afterwards, in order to verify the reliability of our proposed method, we made comparisons with Ref. [42], where the same film-substrate under same loading condition is considered. The resultant film-substrate interface stress profiles are shown in Fig. 5, it can be concluded from Fig. 5 that our method are reliable for calculating the elastic fields.

Hertz load acting on top surface plane of isotropic elastic film on rigid substrate is simulated, as described by Eq. (4), where the contact radius $a = 10$ nm, and Hertz stress amplitude $P_0 = 5$ GPa. The material of thin film is Cu, with its Voigt isotropic modulus shown in Table 1. The geometrical parameters of thin film is: thickness $h$=20 mm, and the stress field within the cross-section of elastic film space is plotted with physical scale along $x$ direction $L_x = 100$ nm and physical scale along $z$ direction $z_0 = 20$ nm. The periodic Fourier transformation wave number is $k_x = k_y = 30$. The produced stress fields under normal traction Hertz load are: Fig. 6a for $\sigma_{xz}$, Fig. 6b for $\sigma_{zz}$, Fig. 6c for $u_x$ and Fig. 6d for $u_z$, respectively.

Hertz load acting on top surface plane of isotropic elastic film-substrate system with imperfect linear-spring interface model is simulated, as described by Eq. (4), where the contact radius $a = 5$ nm, and Hertz stress amplitude $P_0 = 5$ GPa. The material of thin film is Cu and the substrate is Nb, with their Voigt isotropic modulus shown in Table 1. The stress field within the cross-section of film-substrate system is plotted with physical scale along $x$ direction $L_x = 100$ nm and physical scale along $z$ direction $z_0 = 40$ nm, including 10 nm thin film and 30 nm substrate along $z$ direction. The linear-spring interface related matrixes $\boldsymbol{K}_T = \text{DIA}[0.2 \quad 0.2]$ and $K_N = 0.2$ are set as

**Table 1** Elastic properties of Cu and Nb

| Materials | $C_{11}$ (GPa) | $C_{12}$ (GPa) | $C_{44}$ (GPa) | Voigt shear modulus (GPa) | Voigt Poison's ratio |
|---|---|---|---|---|---|
| Cu | 168.4 | 121.4 | 75.4 | 54.64 | 0.3241 |
| Nb | 240.2 | 125.6 | 28.2 | 39.84 | 0.3875 |

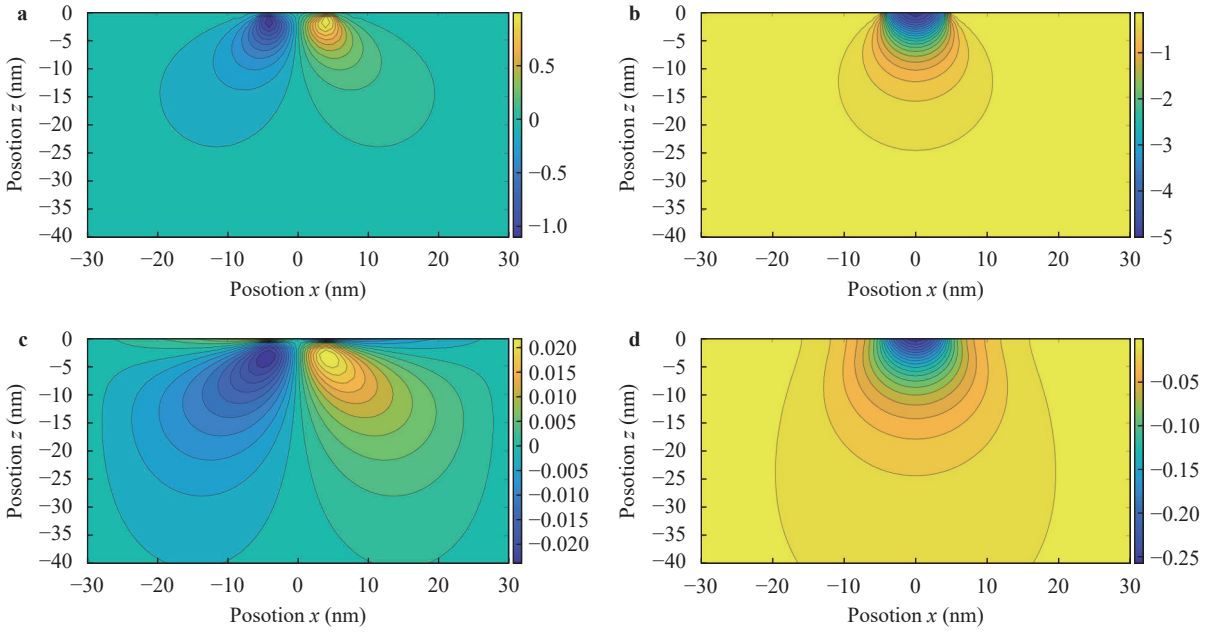


**Fig. 2.** Resultant stress (unit: GPa) of isotropic half space under normal Hertz load: **a** $T_{xz}$, **b** $T_{zz}$ and resultant displacement (unit: nm): **c** $u_x$, **d** $u_z$ within half space.

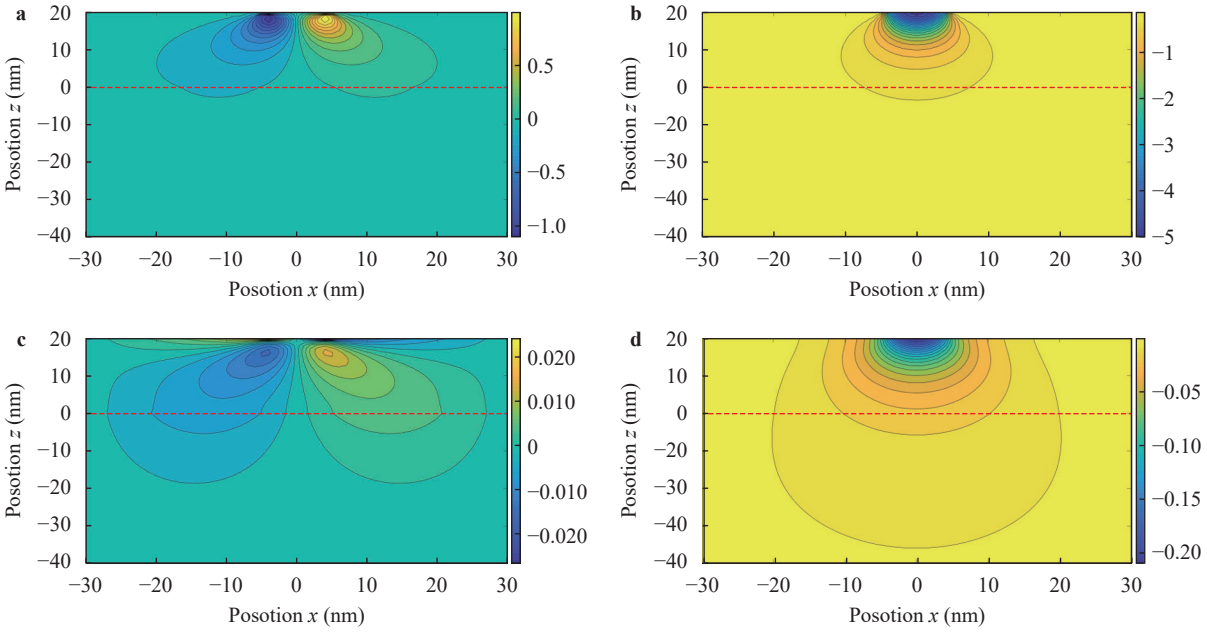


**Fig. 3.** Resultant stress (unit: GPa) of elastic film-substrate system under Hertz load: **a** $T_{xz}$, **b** $T_{zz}$ and resultant displacement (unit: nm): **c** $u_x$, **d** $u_z$ within film-substrate system.

constant for describing the interface imperfection. The periodic Fourier transformation wave number is $k_x = k_y = 30$. The produced stress fields under normal traction Hertz load are: Fig. 7a for $\sigma_{xz}$, Fig. 7b for $\sigma_{zz}$, Fig. 7c for $u_x$ and Fig. 7d for $u_z$, respectively. Comparisons of interface traction and displacement profiles along $x$ direction in the $xz$ plane ($y$=0) are shown in Fig. 8.

Hertz load cting on top surface plane of isotropic elastic film-substrate system with imperfect dislocation-like interface model is simulated, as described by Eq. (4), where the contact radius $a = 5$ nm, and Hertz stress amplitude $P_0 = 5$ GPa. The material of thin film is Cu and the substrate is Nb, with their Voigt isotropic modulus shown in Table 1. The stress field within the cross-section of film-substrate system is plotted with physical scale along $x$ direction $L_x = 100$ nm and physical scale along $z$

direction $z_0 = 40$ nm, including 10 nm thin film and 30 nm substrate along z direction. The dislocation-like interface related matrixes $\boldsymbol{K}^u = \mathrm{DIA}[0.5 \quad 0.5 \quad 0.5]$ are set as constant for describing the interface imperfection. The periodic Fourier transformation wave number is $k_x = k_y = 30$. The produced stress fields under normal traction Hertz load are: Fig. 9a for $\sigma_{xz}$, Fig. 9b for $\sigma_{zz}$, Fig. 9c for $u_x$ and Fig. 9d for $u_z$, respectively. Comparisons of interface traction and displacement profiles along $x$ dir-

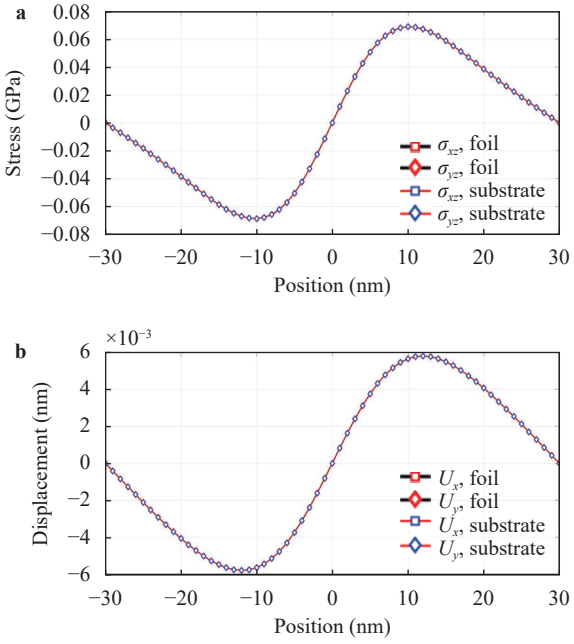


**Fig. 4.** Comparisons of Hertz load induced interface elastic profiles within elastic film-substrate system: **a** stress and **b** displacement.

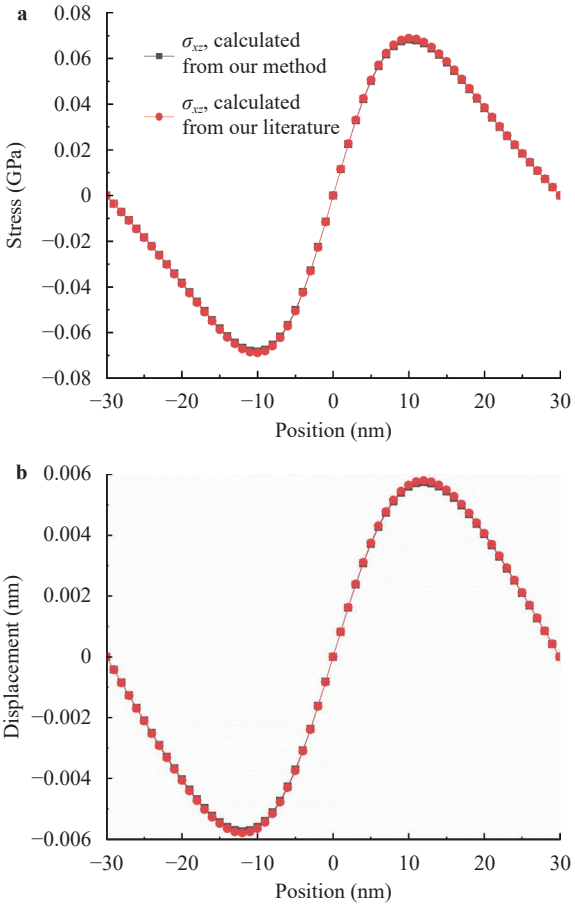


**Fig. 5.** Verification of our methods with classic method in Ref. [42] for film-substrate system under Hertz load, interface elastic profiles within elastic film-substrate system: **a** stress and **b** displacement.

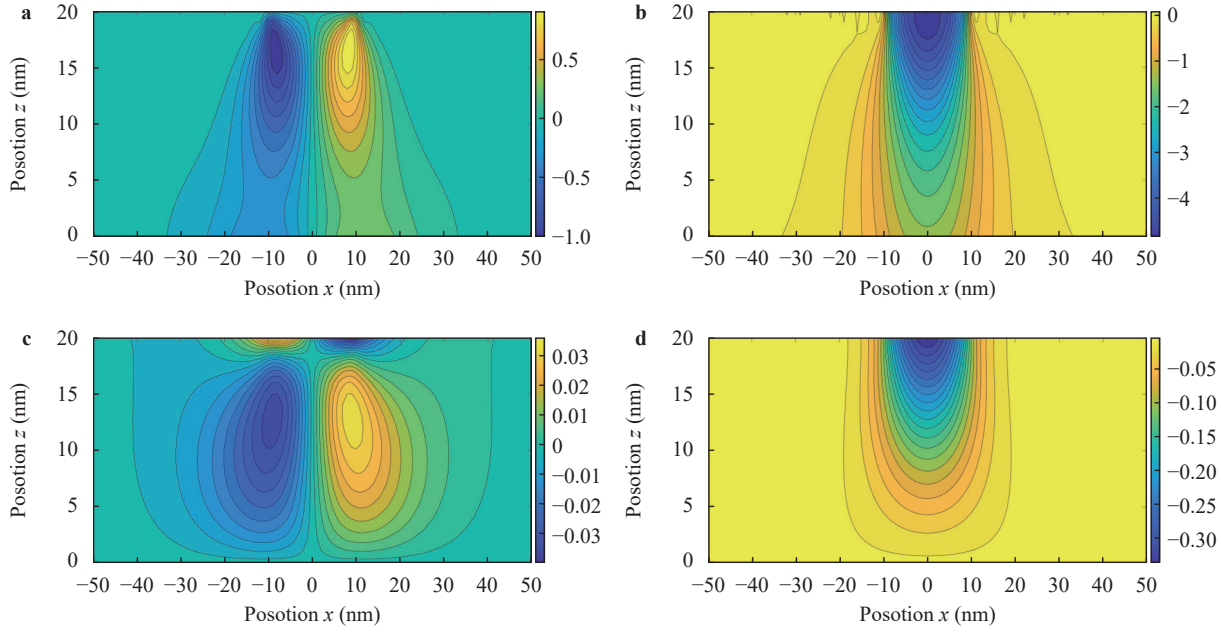


**Fig. 6.** Resultant stress (unit: GPa) of thin film within elastic film rigid substrate system under normal Hertz load: **a** $T_{xz}$, **b** $T_{zz}$ and resultant displacement (unit: nm): **c** $u_x$, **d** $u_z$ within elastic film space.

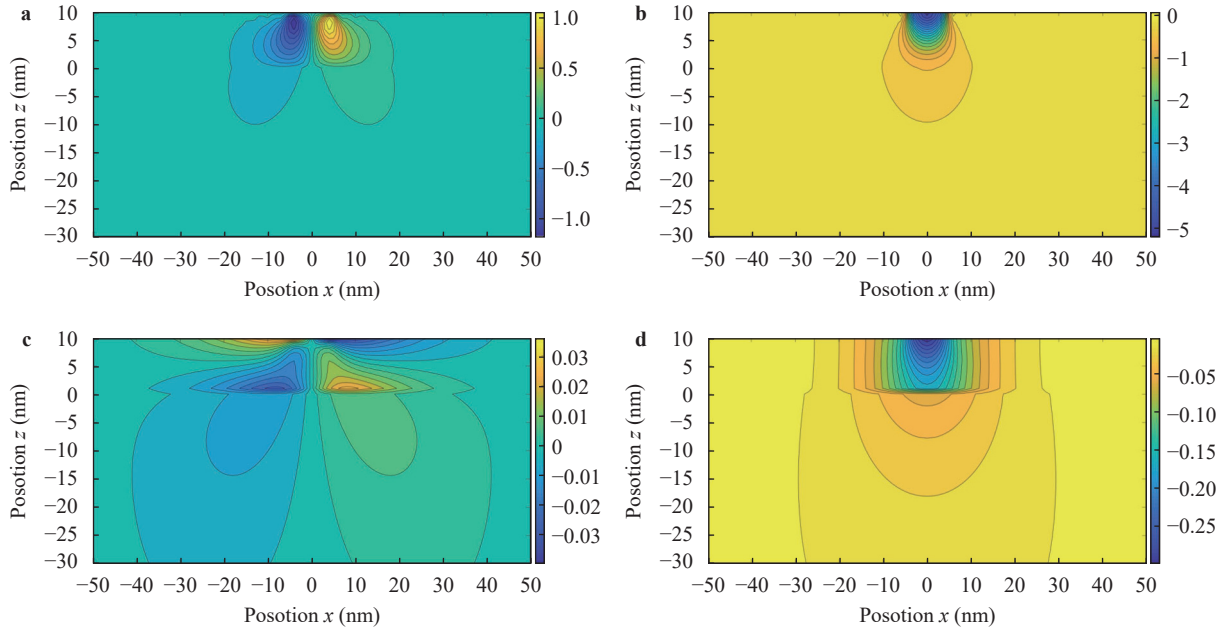


**Fig. 7.** Resultant stress (unit: GPa) of elastic film-substrate system with linear spring-like interface under normal Hertz load: **a** $T_{xz}$, **b** $T_{zz}$ and resultant displacement (unit: nm): **c** $u_x$, **d** $u_z$ within thin film-substrate space.

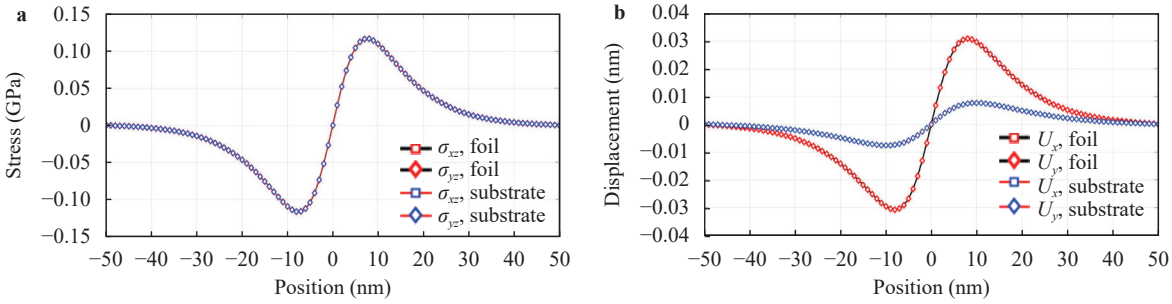


**Fig. 8.** Comparisons of Hertz load induced interface elastic profiles within elastic film-substrate systemwith linear-spring interface: **a** stress and **b** displacement.

ection in the $xz$ plane ($y$=0) are shown in Fig. 10.

Hertz load acting on top surface plane of isotropic elastic film-substrate system with imperfect force-like interface model is simulated, as described by Eq. (4), where the contact radius $a = 5$ nm, and Hertz stress amplitude $P_0 = 5$ GPa. The material of thin film is Cu and the substrate is Nb, with their Voigt isotropic modulus shown in Table 1. The stress field within the cross-section of film-substrate system is plotted with physical scale along $x$ direction $L_x = 100$ nm and physical scale along $z$ direction $z_0 = 40$ nm, including 10 nm thin film and 30 nm substrate along z direction. The force-like interface related matrixes $\boldsymbol{K}^t = \mathrm{DIA}[0.5 \quad 0.5 \quad 0.5]$ are set as constant for describing the interface imperfection. The periodic Fourier transformation wave number is: $k_x = k_y = 30$. The produced stress fields under normal traction Hertz load are: Fig. 11a for $\sigma_{xz}$, Fig. 11b for $\sigma_{zz}$, Fig. 11c for $u_x$and Fig. 11d for $u_z$, respectively. Comparisons of interface traction and displacement profiles along $x$ direction in the $xz$ plane ($y$=0) are shown in Fig. 12.

Based on discrete Fourier transformation of elastic boundary load fields, efficient calculation methods for analyzing the deformation fields of half space, film-substrate system and film on rigid substrate systems are explored. Classic Hertz load examples are performed for verification. Afterwards, the method is extend for film-substrate system with imperfect interface continuity cases, and three classic interface models are considered: (1) the spring-like imperfect interface model which can be described as: $u_k^f\big|_{z^f=-h} - u_k^s\big|_{z^s=0} = \boldsymbol{K}_T \sigma_{kz}$ and $u_z^f\big|_{z^f=-h} - u_z^s\big|_{z^s=0} = \boldsymbol{K}_N \sigma_{zz}$; (2) the dislocation-like interface model, where interface displacement and stress components relation can be described as: $u_i^f\big|_{z^f=0} = \boldsymbol{k}_{ij}^u \; u_i^s\big|_{z^s=0}$ and $\sigma_{iz}^f\big|_{z^f=0} = \sigma_{iz}^s\big|_{z^s=0}$; (3) the force-like interface model, where interface displacement and stress components relation can be described as: $u_i^f\big|_{z^f=0} = u_i^s\big|_{z^s=0}$ and $\sigma_{iz}^f\big|_{z^f=0} = \boldsymbol{k}_{ij}^t \; \sigma_{iz}^s\big|_{z^s=0}$, respectively. The proposed novel calculation methods can be further developed for anisotropic film-substrate systems, functionally graded systems.

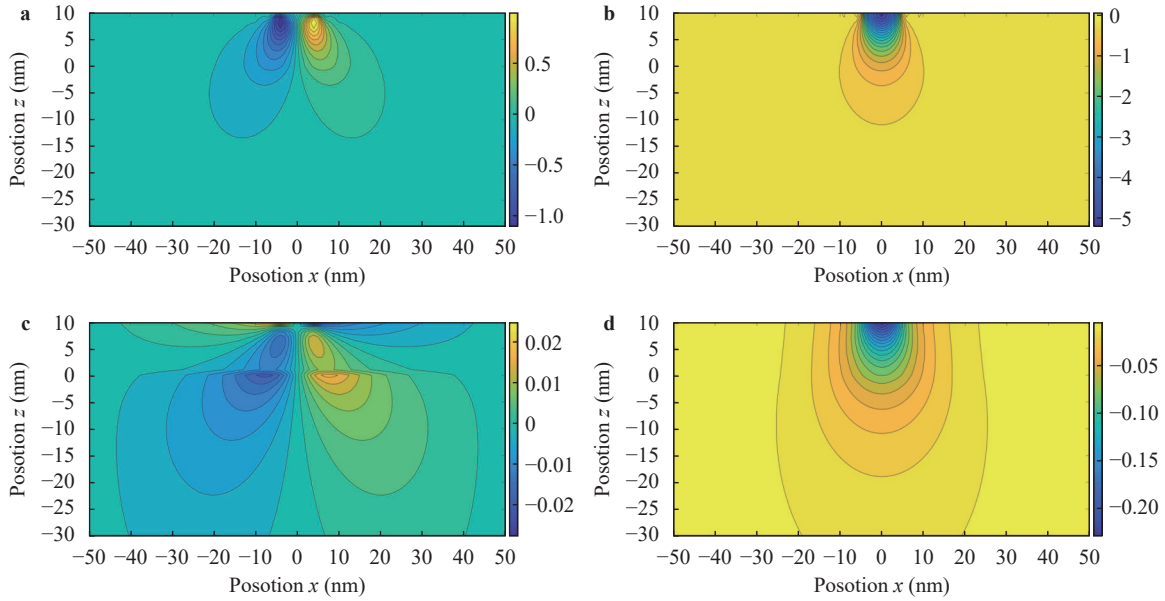


**Fig. 9.** Resultant stress (unit: GPa) of film-substrate system with dislocation-like interface under normal Hertz load: **a** $T_{xz}$, **b** $T_{zz}$ and resultant displacement (unit: nm): **c** $u_x$, **d** $u_z$ within thin film-substrate space.

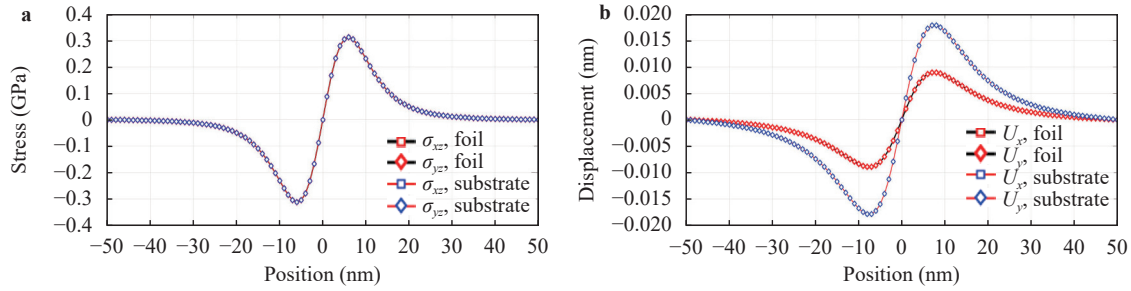


**Fig. 10.** Comparisons of Hertz load induced interface elastic profiles within film-substrate system with dislocation-like interface: **a** stress and **b** displacement.

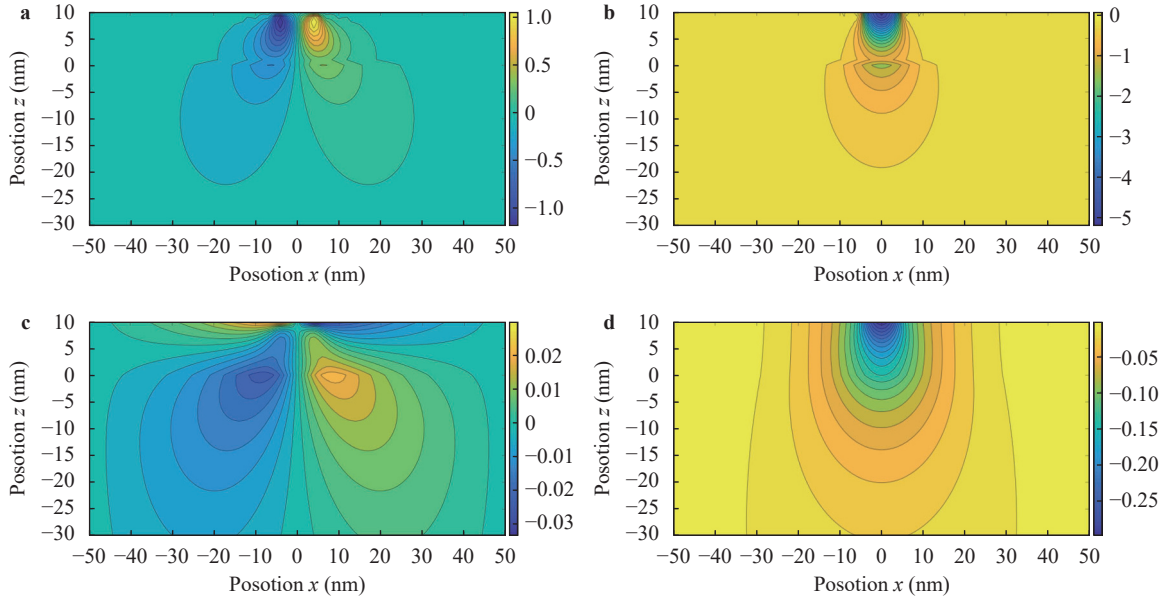


**Fig. 11.** Resultant stress (GPa) of film-substrate system with force-like interface under normal Hertz load: **a** $T_{xz}$, **b** $T_{zz}$ and resultant displacement (unit: nm): **c** $u_x$, **d** $u_z$ within thin film-substrate space.

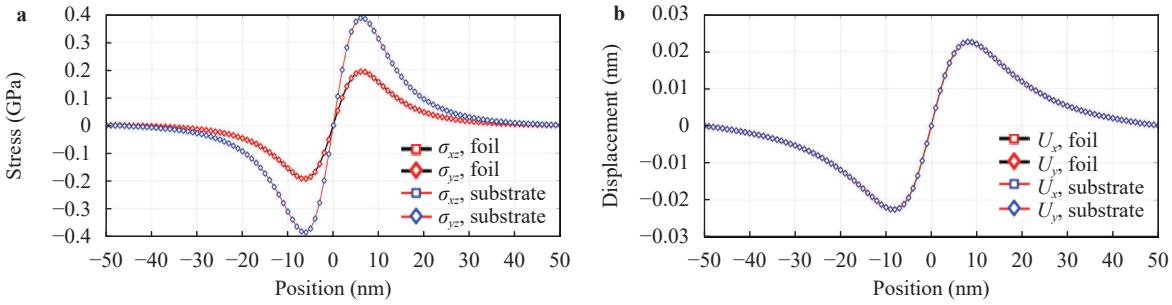


**Fig. 12.** Comparisons of Hertz load induced interface elastic profiles of elastic film-substrate system with force-like interface: **a** stress and **b** displacement.

**Acknowledgement**

This work was supported by the National Natural Science Foundation of China (Grants 11702023 and 11972081).

**References**

[1] L.J. Sudak, X. Wang, Green's function in plane anisotropic bimaterials with imperfect interface, IMA Journal of Applied Mathematics 71 (2006) 783–794.
[2] E. Pan, Three-dimensional Green's functions in anisotropic elastic bimaterials with imperfect interfaces, Journal of Applied Mechanics-Transactions of the ASME 70 (2003) 180–190.
[3] J. Dundurs, M. Hetenyi, Transmission of force between two semi-infinite solids, Journal of Applied Mechanics-Transactions of the ASME 32 (1965) 671–674.
[4] Z. Hashin, Thin interphase/imperfect interface in conduction, Journal of Applied Physics 89 (2001) 2261–2267.
[5] Y. Benveniste, On the decay of end effects in conduction phenomena: a sandwich strip with imperfect interfaces of low or high conductivity, J. App. Phy. 86 (1999) 1273–1279.
[6] L.E. Shilkrot, D.J. Srolovitz, Elastic analysis of finite stiffness bimaterial interfaces: application to dislocation-interface interactions, Acta Materialia 46 (1998) 3063–3075.
[7] H.Y. Yu, S.C. Sanday, Elastic fields in joined half-spaces due to nuclei of strain, Proceedings of the Royal Society of London. Series A 434 (1991) 503–519.
[8] H.Y. Yu, S.C. Sanday, B.B. Rath, et al., Elastic fields due to defects in transversely isotropic bimaterials, Proceedings of the Royal Society of London. Series A 449 (1995) 1–30.
[9] E. Pan, F.G. Yuan, Three-dimensional Green's functions in anisotropic bimaterials, International Journal of Solids and Structures 37 (2000) 5329–5351.
[10] Y. Benveniste, T. Chen, On the Saint-Venant torsion of composite bars with imperfect interfaces, Proceedings of the Royal Society of London. Series A 457 (2001) 231–255.
[11] H.Y. Yu, A new dislocation-like model for imperfect interfaces and their effect on load transfer, Composites Part A-Applied Science and Manufacturing 29 (1998) 1057–1062.
[12] T. Mura, R. Furuhashi, The elastic inclusion with a sliding interface, J. App. Mech.-Trans. ASME 51 (1984) 308–310.
[13] W.T. Chen, Computation of stresses and displacements in a layered elastic medium, International Journal of Engineering Science 9 (1971) 775–800.
[14] W.T. Chen, P.A. Engel, Impact and contact stress analysis in multilayer media, Inter. J. Solids Struct. 8 (1972) 1257–1281.
[15] Z. Hashin, Thermoelastic properties of fiber composites with imperfect interface, Mechanics of Materials 8 (1990) 333–348.
[16] J.D. Achenbach, H. Zhu, Effect of interfacial zone on mechanical behavior and failure of fiber-reinforced composites, Journal of the Mechanics and Physics of Solids 37 (1989) 381–393.
[17] J. Qu, The effect of slightly weakened interfaces on the overall elastic properties of composite materials, Mech. Mater. 14 (1993) 269–281.
[18] W.Y. Yang, Q.H. Zhou, Y.Y. Huang, et al., A thermoelastic contact model between a sliding ball and a stationary half space distributed with spherical inhomogeneities, Tribology International 131 (2019) 33–44.
[19] Z.J. Wang, C.J. Yu, Q.J. Wang, An efficient method for solving three-dimensional fretting contact problems involving multilayered or functionally graded materials, International Journal of Solids and Structures 66 (2015) 46–61.
[20] X. Zhang, Z.J. Wang, H.M. Shen, et al., An efficient model for the frictional contact between two multiferroic bodies, International Journal of Solids and Structures 130-131 (2018) 133–152.
[21] H. Yu, Z.J. Wang, Q.J. Wang, Analytical solutions for the elastic fields caused by eigenstrains in two frictionlessly joined half-spaces, Inter. J. Solids Struct. 100-101 (2016) 74–94.
[22] X. Zhang, Q.J. Wang, Y.X. Wang, et al., Contact involving a functionally graded elastic thin film and considering surface effects, Inter. J. Solids Struct. 150 (2018) 184–196.
[23] D. L. Li, Z. J. Wang, H. Yu, et al., Elastic fields caused by eigenstrains in two joined half-spaces with an interface of coupled imperfections: dislocation-like and force-like conditions, International Journal of Engineering Science 126 (2018) 22–52.
[24] X. Zhang, Z.J. Wang, H.M. Shen, et al., Frictional contact involving a multiferroic thin film subjected to surface magneto-electroelastic effects, International Journal of Mechanical Sciences 131-132 (2017) 633–648.
[25] Z.J. Wang, H. Yu, Q.J. Wang, Layer-substrate system with an imperfectly bonded interface: coupled dislocation-like and force-like conditions, International Journal of Solids and Structures 122- 123 (2017) 91–109.
[26] Z.J. Wang, H. Yu, Q.J. Wang, Layer-substrate system with an imperfectly bonded interface: spring-like condition, International Journal of Mechanical Sciences 134 (2017) 315–335.
[27] H.Y. Yu, Y.N. Wei, F.P. Chiang, Load transfer at imperfect interfaces - dislocation-like model, International Journal of Engineering Science 40 (2002) 1647–1662.
[28] I.A. Polonsky, L.M. Keer, A numerical method for solving rough contact problems based on the multi-level multi-summation and conjugate gradient techniques, Wear 231 (1999) 206–219.

[29] Y.Q. Liu, W.Z. Wang, H.B. Zhang, et al., Solution of temperature distribution under frictional heating with consideration of material inhomogeneity, Tribology Inter. 126 (2018) 80–96.
[30] H.B. Zhang, W.Z. Wang, S.G. Zhang, et al., Semi-analytical solution of three-dimensional steady state thermoelastic contact problem of multilayered material under friction heating, International Journal of Thermal Sciences 127 (2018c) 384–399.
[31] H.B. Zhang, W.Z. Wang, S.G. Zhang, et al., Semi-analytic solution of three-dimensional temperature distribution in multilayered materials based on explicit frequency response functions, Inter. J. Heat Mass Trans. 118 (2018d) 208–222.
[32] W. Wu, R. Schäublin, J. Chen, General dislocation image stress of anisotropic cubic thin film, Journal of Applied Physics 112 (2012) 093522.
[33] W. Wu, R. Xia, G. Qian, et al., Edge-on dislocation loop in anisotropic hcp zirconium thin foil, Journal of Nuclear Materials 465 (2015) 212–223.
[34] W. Wu, R. Xia, S. Xu, et al., Elastic field of approaching dislocation loop in isotropic biomaterial, Modelling and Simulation in Materials Science and Engineering 23 (2015) 075006.
[35] W. Wu, C. Lv, J. Zhang, Interface traction stress of dislocation loop in anisotropic biomaterial, Journal of the Mechanics and Physics of Solids 87 (2015c) 7–37.
[36] W. Wu, S. Xu, C. Lv, et al., Dislocation loop in isotropic bimaterial with linear spring-like imperfect interface, Journal of Applied Mechanics-Transactions of the ASME 83 (2016) 041005.
[37] W. Wu, C. Lv, S. Xu, et al., Elastic field due to dislocation loops in isotropic bimaterial with dislocation-like and force-like interface models, Mathematics and Mechanics of Solids 22 (2017) 1190–1204.
[38] R. Xia, W. Wu, R. Wu, Elastic field due to dislocation loops in isotropic multilayer system, Journal of Mechanical Science and Technology 51 (2016) 2942–2957.
[39] W. Wu, R. Schaeublin, The elasticity of the ½ $a_0$ <111> and $a_0$ <100> dislocation loop in α-Fe thin foil, Journal of Nuclear Materials 510 (2018) 61–69.
[40] A.F. Bower, Applied Mechanics of Solids, CRC Press London (2012).
[41] W. Voigt, Ueber die Beziehung zwischen den beiden elasticitätsconstanten isotroper körper, Annals of Physics 274 (1889) 573–587.
[42] N. Schwarzer, F. Richter, G. Hecht, The elastic field in a coated half-space under Hertzian pressure distribution, Surface and Coatings Technology 114 (1999) 292–304.

## Appendix

$$\boldsymbol{D}^s = \begin{bmatrix} +n_x z^s & -n_y & +\mathrm{i}n_x \\ +n_y z^s & +n_x & +\mathrm{i}n_y \\ +\mathrm{i}\dfrac{\lambda^s+3\mu^s}{\lambda^s+\mu^s} - \mathrm{i}n_z z^s & 0 & +n_z \end{bmatrix} \exp\left(+n_z z^s\right), \tag{A1}$$

$$\boldsymbol{T}^s = \begin{bmatrix} +\mu^s\left(-n_x\dfrac{2\mu^s}{\lambda^s+\mu^s}+2n_x n_z z^s\right) & -n_y n_z\mu^s & +2\mathrm{i}n_x n_z\mu^s \\ +\mu^s\left(-n_y\dfrac{2\mu^s}{\lambda^s+\mu^s}+2n_y n_z z^s\right) & +n_x n_z\mu^s & +2\mathrm{i}n_y n_z\mu^s \\ +2\mathrm{i}n_z\dfrac{\mu^s}{\lambda^s+\mu^s}\left(\lambda^s+2\mu^s\right)-2\mathrm{i}n_z n_z\mu^s z^s & 0 & +2n_z n_z\mu^s \end{bmatrix} \exp\left(+n_z z^s\right), \tag{A2}$$

$$\boldsymbol{D}^{\mathrm{syym}} = \begin{bmatrix} n_x h\sinh(n_z h) & n_y\cosh(n_z h) & \mathrm{i}n_x\cosh(n_z h) \\ n_y h\sinh(n_z h) & -n_x\cosh(n_z h) & \mathrm{i}n_y\cosh(n_z h) \\ -\mathrm{i}n_z h\cosh(n_z h)+\mathrm{i}\dfrac{\lambda^f+3\mu^f}{\lambda^f+\mu^f}\sinh(n_z h) & 0 & n_z\sinh(n_z h) \end{bmatrix}, \tag{A3}$$

$$\boldsymbol{D}^{\mathrm{assym}} = \begin{bmatrix} n_x h\cosh(n_z h) & -n_y\sinh(n_z h) & \mathrm{i}n_x\sinh(n_z h) \\ n_y h\cosh(n_z h) & n_x\sinh(n_z h) & \mathrm{i}n_y\sinh(n_z h) \\ -\mathrm{i}n_z h\sinh(n_z h)+\mathrm{i}\dfrac{\lambda^f+3\mu^f}{\lambda^f+\mu^f}\cosh(n_z h) & 0 & n_z\cosh(n_z h) \end{bmatrix}, \tag{A4}$$

$$\boldsymbol{T}^{\mathrm{syym}} = \begin{Bmatrix} 2\mu^f n_x\left[n_z h\cosh(n_z h)-\dfrac{\mu^f}{\lambda^f+\mu^f}\sinh(n_z h)\right] & \mu^f n_y n_z\sinh(n_z h) & 2\mathrm{i}\mu^f n_x n_z\sinh(n_z h) \\ 2\mu^f n_y\left[n_z h\cosh(n_z h)-\dfrac{\mu^f}{\lambda^f+\mu^f}\sinh(n_z h)\right] & -\mu^f n_x n_z\sinh(n_z h) & 2\mathrm{i}\mu^f n_y n_z\sinh(n_z h) \\ 2\mathrm{i}\mu^f\left[\dfrac{\lambda^f+2\mu^f}{\lambda^f+\mu^f}n_z\cosh(n_z h)-n_z^2 h\sinh(n_z h)\right] & 0 & 2\mu^f n_z^2\cosh(n_z h) \end{Bmatrix}, \tag{A5}$$

$$\boldsymbol{T}^{\text{assym}} = \left\{ \begin{array}{ccc} 2\mu^f n_x \left[ n_z h \sinh(n_z h) - \dfrac{\mu^f}{\lambda^f + \mu^f} \cosh(n_z h) \right] & -\mu^f n_y n_z \cosh(n_z h) & 2\mathrm{i}\mu^f n_x n_z \cosh(n_z h) \\ 2\mu^f n_y \left[ n_z h \sinh(n_z h) - \dfrac{\mu^f}{\lambda^f + \mu^f} \cosh(n_z h) \right] & \mu^f n_x n_z \cosh(n_z h) & 2\mathrm{i}\mu^f n_y n_z \cosh(n_z h) \\ 2\mathrm{i}\mu^f \left[ \dfrac{\lambda^f + 2\mu^f}{\lambda^f + \mu^f} n_z \sinh(n_z h) - n_z^2 h \cosh(n_z h) \right] & 0 & 2\mu^f n_z^2 \sinh(n_z h) \end{array} \right\}. \tag{A6}$$